Journal of Solid State Chemistry 225 (2015) 65–71

Contents lists available at ScienceDirect

Journal of Solid State Chemistry

journal homepage: www.elsevier.com/locate/jssc

Synthesis and crystal structure analysis of $Li_2NaBP_2O_8$ and $LiNa_2B_5P_2O_{14}$

Toru Hasegawa, Hisanori Yamane *

Institute of Multidisciplinary Research for Advanced Materials, Tohoku University, 2-1-1 Katahira, Aoba-ku, Sendai 980-8577, Japan

ARTICLE INFO

Article history:
Received 27 September 2014
Received in revised form
17 November 2014
Accepted 27 November 2014
Available online 8 December 2014

Keywords:
Borophosphate
Solid-state reaction
Crystal structure

ABSTRACT

Single crystals of $Li_2NaBP_2O_8$ and $LiNa_2B_5P_2O_{14}$ were prepared at 873–883 K. The XRD reflections of $Li_2NaBP_2O_8$ single crystal were indexed with triclinic unit-cell parameters of $a=5.4344(3)$ Å, $b=7.3793(4)$ Å, $c=7.9840(4)$ Å, $\alpha=103.243(3)^\circ$, $\beta=109.270(4)^\circ$ and $\gamma=87.391(2)^\circ$; (space group $P\bar{1}$ (No. 2)). $Li_2NaBP_2O_8$ consists of one-dimensional $^1_\infty[BP_2O_8]^{3-}$ chains of BO_4 and PO_4 tetrahedra in the direction of the c axis, and Li and Na atoms located around the chains. The XRD reflections of the $LiNa_2B_5P_2O_{14}$ single crystal were indexed with monoclinic unit-cell parameters of $a=8.208(3)$ Å, $b=9.151(3)$ Å, $c=8.349(3)$ Å and $\beta=115.709(7)^\circ$; (space group $P2_1/m$ (No. 11)). In the crystal structure of $LiNa_2B_5P_2O_{14}$, BO_3 trigonal planer and BO_4 and PO_4 tetrahedra share O atoms and form two-dimensional sheets of $^2_\infty[B_5P_2O_{14}]^{3-}$. One Li and two Na atoms are situated at a large triangular space in the sheets.

1. Introduction

Borophosphates have been actively synthesized and researched for more than twenty years [1–5]. Based on the rich structural chemistry of borophosphate anions, which extends from isolated species, oligomers, rings and chains to layers and frameworks, potential applications of borophosphates have received considerable attention. Concepts for the classification of crystalline borophosphates in terms of structural chemistry by the B:P ratio, bonding mode of BO_3, BO_4 and PO_4 and their dimensionalities have been proposed [2–4].

Recently, we attempted preparation of single crystals to analyze the crystal structures of $Li_{22}B_{11}P_{13}O_{60}$ and $Li_2B_3PO_8$ reported by Tien and Hummel [6]. Crystal structure analysis by X-ray diffraction (XRD) revealed that $Li_{22}B_{11}P_{13}O_{60}$ is $Li_3BP_2O_8$ (triclinic; (space group $P\bar{1}$ (No. 2)) $a=5.1888(5)$ Å, $b=7.4118(7)$ Å, $c=7.6735(7)$ Å, $\alpha=101.179(3)^\circ$, $\beta=105.067(3)^\circ$ and $\gamma=90.335(3)^\circ$) [7]. One-dimensional $^1_\infty[BP_2O_8]^{3-}$ chains were found to form in the direction of the c axis by linking the four-membered rings composed of two PO_4 and two BO_4 tetrahedra in $Li_3BP_2O_8$. The ionic conductivity measured for the polycrystalline $Li_3BP_2O_8$ bulk sample was 1.5×10^{-5} S cm^{-1} at 583 K. In the crystal structure of $Li_2B_3PO_8$, Li ions were found to be in the space of $^2_\infty[B_3PO_8]^{2-}$ sheets formed by the linkage of triangular BO_3 and tetrahedral BO_4 and PO_4 groups. This structure is the first example of two-dimensional borophosphate sheets which consist of a mixture of triangular and tetrahedral BO_4 and tetrahedral PO_4 groups [8].

The crystal structure of $Na_5B_2P_3O_{13}$ was reported by Hauf et al. [9,10]. One-dimensional $^1_\infty[B_2P_3O_{13}]^{5-}$ chains are formed in the [0 0 1] direction of this structure by sharing O atoms of PO_4 and BO_4 tetrahedra. $Na_5B_2P_3O_{13}$ has been synthesized by the hydrothermal method [10]. Moreover, $Na_5B_2P_3O_{13}$ has been studied as a nonlinear optical material, and synthesis of large size single crystals by the Czochralski method and by a heat exchanger method has also been performed [11,12]. According to the crystal structure analysis of $Na_3B_6PO_{13}$ by Xiang et al. [13], $Na_3B_6PO_{13}$ contains one-dimensional $^1_\infty[BP_6O_{13}]^{3-}$ chains with eight-membered rings of four PO_4 and four BO_4 tetrahedra. Similar $^1_\infty[BP_2O_8]^{3-}$ chains are contained in $Na_3BP_2O_8$; however, the chains lay across each other in neighboring layers [13].

Many borophosphates reported in recent years have been synthesized under hydrothermal conditions, OH^- and/or H_2O being contained in the structures [4]. $Li_3BP_2O_8$, $Li_2B_3PO_8$ and $Na_5B_2P_3O_{13}$ have been synthesized by solid state reaction, and synthesis of $Na_3B_6PO_{13}$ and $Na_3BP_2O_8$ has been performed by using boric acid and sodium dihydrogen phosphate as flux. These compounds containing no OH^- and H_2O are relatively rare.

Anhydrous and/or anhydrate borophosphates containing two different kinds of alkali metals reported in a previous study are $Li_2Cs_2B_2P_4O_{15}$, $Li_3K_2BP_4O_{14}$, $LiK_2BP_2O_8$ and $Li_3Rb_2BP_4O_{14}$ [14]. But borophosphates containing both Li and Na have not been reported. In the present study, we synthesized $Li_2NaBP_2O_8$ by substituting a part of the Na atom for the Li atom of $Li_3BP_2O_8$. $LiNa_2B_5P_2O_{14}$ was prepared by adding H_3BO_3 to the sample of $Li_2NaBP_2O_8$. The crystal structures of

* Corresponding author. Fax: +81 22 217 5813.
E-mail address: yamane@tagen.tohoku.ac.jp (H. Yamane).

http://dx.doi.org/10.1016/j.jssc.2014.11.024
0022-4596/

these new quintenary compounds were analyzed and their electrical conductivities were characterized.

2. Experimental

H_3BO_3 (99.5%, Wako Pure Chemical Ind.), Li_2CO_3 (99.0%, Wako Pure Chemical Ind.), Na_2CO_3 (99.8%, Wako Pure Chemical Ind.) and $NH_4H_2PO_4$ (99.0%, Wako Pure Chemical Ind.) were used as starting powders. These powders were weighed with a molar ratio of 1/2Li_2CO_3:1/2Na_2CO_3:H_3BO_3:$NH_4H_2PO_4$=1:2:1:2, mixed in an agate mortar with a pestle and pressed into a pellet. The pellet was placed on a platinum plate and heated at 473 K for 9 h in air with an electric furnace. After cooling, the product was powdered, pelletized and heated at 823 K for 12 h. The phases in the obtained polycrystalline sample were identified by powder XRD using Cu$K\alpha$ radiation with a pyrolitic graphite monochromator, a scintillation counter, and a diffractometer (Rigaku, RINT, 40 kV, 30 mA).

The polycrystalline sample was heated again at 873 K for 1 h, and then cooled to 773 K at a rate of −2 K/h. After cooling from 773 K to room temperature in the furnace, the product was crushed and an $Li_2NaBP_2O_8$ single crystal for crystal structure analysis was chosen. Furthermore, the polycrystalline sample (0.0310 g) and H_3BO_3 (0.0308 g) were mixed and pressed into a pellet and heated at 883 K for 1 h, followed by cooling to 783 K at a rate of −10 K/h. The product was crushed and a single crystal of $LiNa_2B_5P_2O_{14}$ was chosen for crystal structure analysis.

A single crystal was fixed to the tip of a glass fiber with epoxy resin and placed in a goniometer of a single-crystal X-ray diffractometer (Rigaku, R-AXIS RAPID-II). X-ray diffraction data of the single crystal were collected using Mo$K\alpha$ radiation with a graphite monochromator and an imaging plate. Unit cell refinement and absorption correction were performed by the programs RAPID-AUTO [15] and NUMABS [16], respectively. All calculations were carried out on a personal computer using the WinGX software package [17]. The crystal structure of $LiNa_2B_5P_2O_{14}$ was obtained by the direct method using the SIR2004 program [18] and structure parameters were refined by the full-matrix least-squares on F^2 using the SHELXL-97 program [19]. Crystal structure illustration and Madelung energy calculation were carried out with the VESTA program [20].

Polycrystalline $Li_2NaBP_2O_8$ bulk samples for electrical conductivity measurement were synthesized with a mixture of Li_2CO_3, Na_2CO_3, H_3BO_3 and $NH_4H_2PO_4$. The powders weighed with a molar ratio of 1/2Li_2CO_3:1/2Na_2CO_3:H_3BO_3:$NH_4H_2PO_4$=2:1:1:2 were mixed, pressed into pellets, and calcined at 423 K for 12 h. The calcined sample was then heated two times at 873 K for 12 h with intermediate pulverization and pelletization. Polycrystalline $LiNa_2B_5P_2O_{14}$ bulk samples were prepared by weighing the starting powder with a molar ratio of Li:Na:B:P=1:2:5:2. The powders were mixed, pressed into pellets, and calcined at 473 K for 12 h. The calcined sample was heated two times at 823 K for 12 h with intermediate pulverization and pelletization.

The electrical conductivity of the polycrystalline bulk samples was measured by the AC impedance method using an impedance analyzer (WAYNE KERR, LCR METER 4100) in a frequency range of 20 Hz–1 MHz in a temperature range of 473–606 K. Graphite paste was used as electrodes.

3. Results and discussion

3.1. Crystal structure of $Li_2NaBP_2O_8$

The XRD reflections of the $Li_2NaBP_2O_8$ single crystal were indexed with triclinic unit-cell parameters of a=5.4344(3) Å, b=7.3793(4) Å, c=7.9840(4) Å, α=103.243(3)°, β=109.270(4)° and γ=87.391(2)°. The space group was given as $P\bar{1}$ (No. 2). $Li_2NaBP_2O_8$ and $Li_3BP_2O_8$ are isotypic. The crystal structure of $Li_2NaBP_2O_8$ was refined with an $R1$-value (2σ) of 2.31%. The results of structure analysis, atomic coordinates, anisotropic displacement parameters and selected bond lengths

Table 1
Crystal data and refinement results for $Li_2NaBP_2O_8$ and $LiNa_2B_5P_2O_{14}$.

Chemical formula	$Li_2NaBP_2O_8$		$LiNa_2B_5P_2O_{14}$	
Formula weight, M_r	237.62 g mol^{-1}		392.91	
Temperature, T	293(2) K		293(2) K	
Crystal system	Triclinic		Monoclinic	
Space group	$P\bar{1}$ (No. 2)		$P2_1/m$ (No. 11)	
Unit cell dimensions	a=5.4344(3) Å	α=103.243(3)°	a=8.208(3) Å	
	b=7.3793(4) Å	β=109.270(4)°	b=9.151(3) Å	β=115.709(7)°
	c=7.9840 (4) Å	γ=87.391(2)°	c=8.349(3) Å	
Unit cell volume, V	294.04(3) Å^3		565.0(3) Å^3	
Z	2		2	
Calculated density, D_{cal}	2.684 Mg m^{-3}		2.309	
Radiation wavelength, λ	0.71075 Å (Mo$K\alpha$)		0.71075	
Crystal form, color	Colorless		Colorless	
Absorption correction	Numerical		Numerical	
Absorption coefficient, μ	0.821 mm^{-1}		0.546	
Crystal size	0.313 × 0.270 × 0.185 mm^3		0.149 × 0.126 × 0.123 mm^3	
Limiting indices	$-7 \le h \le 7$		$-10 \le h \le 10$	
	$-9 \le k \le 9$		$-11 \le k \le 11$	
	$-10 \le l \le 10$		$-10 \le l \le 10$	
F_{000}	232		384	
θ range for data collection	3.49°–27.48°		3.51°–27.48°	
Reflections collected/unique	1338/1217		1350/1098	
R_{int}	0.0128		0.0639	
Data/restraints/parameters	1334/0/127		1350/0/130	
Weight parameters, a, b	0.0397, 0.2198		0.0398, 0.4367	
Goodness-of-fit on F^2, S	1.081		1.059	
$R1$, $wR2$ ($I > 2\sigma(I)$)	0.0231, 0.0651		0.0424, 0.0896	
$R1$, $wR2$ (all data)	0.0256, 0.0669		0.0548, 0.0985	
Largest diff. peak and hole, $\Delta\rho$	0.501, −0.293 e Å^{-3}		0.422, −0.588 e A^{-3}	

$R1=\Sigma||F_o|-|F_c||/\Sigma|F_o|$. $wR2=[\Sigma w(F_o^2-F_c^2)^2/\Sigma(wF_o^2)^2]^{1/2}$, $w=1/[\sigma^2(F_o^2)+(aP)^2+bP]$, where F_o is the observed structure factor, F_c is the calculated structure factor, σ is the standard deviation of F_c^2, and $P=(F_o^2+2F_c^2)/3$. $S=[\Sigma w(F_o^2-F_c^2)^2/(n-p)]^{1/2}$, where n is the number of reflections and p is the total number of parameters refined.

of $Li_2NaBP_2O_8$ are listed in Tables 1–4. Fig. 1 shows the coordination environment around metal atoms of $Li_2NaBP_2O_8$ using the structural parameters.

B, P1 and P2 atoms are coordinated by four O atoms and form boron/phosphorus atom-centered oxygen tetrahedra, Li1 and Li2 atoms are coordinated by four O atoms and Na1 atoms by five. The B1–O distances vary from 1.459(2) to 1.486(2) Å, P1–O distances from 1.4937(12) to 1.5740(12) Å, P2–O distances from 1.4964(12) to 1.5807(17) Å, Li1–O distances from 1.907(3) to 1.981(3) Å, Li2–O distances from 1.873(3) to 2.071(4) Å and Na1–O distances from 2.3492(14) to 2.4543(14) Å. The bond valence sums (BVS) for the atoms were calculated with the bond lengths and the bond valence parameters l_0 ((Li^+)=1.466 Å, (Na^+)=1.803 Å, (B^{3+})=1.371 Å, (P^{5+})=1.617 Å) presented by Brece and O'Keeffe [21]. The BVSs were Li1:1.08, Li2:1.02, Na:0.96, B: 3.05, P1: 4.98 and P2: 4.97, respectively. These values are consistent with the valences of the elements.

The value of the Madelung part of lattice energy (MAPLE) for $Li_2NaBP_2O_8$ calculated with the structure parameters was −60,500 kJ/mol, which was almost identical to the value of −59,600 kJ/mol (difference Δ=1.5%) of the MAPLEs: Li_2O −3500 kJ/mol [22], Na_2O −2900 kJ/mol [23], B_2O_3 −21,900 kJ/mol [24], and P_2O_5 −43,700 kJ/mol [25] with the formula of $Li_2NaBP_2O_8$=Li_2O+1/2 Na_2O+1/2 B_2O_3+P_2O_5.

Figs. 2 and 3 show the crystal structures $Li_2NaBP_2O_8$ and $Li_3BP_2O_8$ in the *a*-axis direction. All oxygen atoms of the BO_4 tetrahedron are shared by four PO_4 tetrahedra in both structures. One-dimensional $^1_\infty[BP_2O_8]^{3-}$ chains are formed in the direction of the *c* axis by linkage

Table 2
Atomic coordinates and isotropic and equivalent isotropic displacement parameters (U_{eq}) for $Li_2NaBP_2O_8$.

Atom	Site	*x*	*y*	*z*	U_{eq}[a] (Å^2)
Li1	2*i*	0.6900(6)	0.4977(4)	0.1418(4)	0.0155(6)
Li2	2*i*	0.1455(6)	0.5323(4)	0.4020(4)	0.0171(6)
Na1	2*i*	0.74671(14)	0.11920(11)	0.25826(11)	0.02093(19)
B1	2*i*	0.2505(3)	0.9526(2)	0.2340(2)	0.0090(3)
P1	2*i*	0.37686(8)	0.22667(5)	0.54715(5)	0.00755(12)
P2	2*i*	0.14608(8)	0.24889(5)	0.05412(5)	0.00726(12)
O1	2*i*	0.0312(2)	0.81837(16)	0.14920(16)	0.0109(2)
O2	2*i*	0.4984(2)	0.13952(16)	0.71772(16)	0.0105(2)
O3	2*i*	0.9876(2)	0.33397(16)	0.17414(16)	0.0116(3)
O4	2*i*	0.1985(2)	0.37707(16)	0.59626(16)	0.0111(2)
O5	2*i*	0.2757(2)	0.06531(15)	0.10798(16)	0.0100(2)
O6	2*i*	0.3561(2)	0.37424(16)	0.05578(16)	0.0123(3)
O7	2*i*	0.1985(2)	0.06661(15)	0.39521(15)	0.0098(2)
O8	2*i*	0.5829(2)	0.28755(16)	0.48409(16)	0.0124(3)

[a] U_{eq}=($\sum_i \sum_j U_{ij} a_i^* a_j^* a_i \cdot a_j$)/3.

Table 4
Selected bond lengths and bond valence sums (V_i) for $Li_2NaBP_2O_8$.

Li1–O6	1.907(3)	Li2–O8^{ii}	1.873(3)
Li1–O3	1.957(3)	Li2–O4^{iii}	1.960(3)
Li1–O6^{i}	1.961(3)	Li2–O3^{iv}	2.013(3)
Li1–O4^{ii}	1.981(3)	Li2–O4	2.071(4)
V_{Li1}	1.08	V_{Li2}	1.02
Na1–O8	2.3492(14)	B1–O1^{ii}	1.459(2)
Na1–O7^{v}	2.3897(14)	B1–O2	1.470(2)
Na1–O3	2.4359(14)	B1–O7^{vi}	1.472(2)
Na1–O5	2.4487(14)	B1–O5^{vi}	1.486(2)
Na1–O2^{vi}	2.4543(14)	V_{B1}	3.05
V_{Na1}	0.96		
P1–O8	1.4937(12)	P2–O6	1.4964(12)
P1–O4	1.5093(12)	P2–O3^{iv}	1.5079(18)
P1–O2	1.5727(12)	P2–O1^{vii}	1.5669(18)
P1–O7	1.5740(12)	P2–O5	1.5807(17)
V_{P1}	4.98	V_{P2}	4.97

Symmetry codes: (i) −*x*+1, −*y*+1, −*z*; (ii) −*x*+1, −*y*+1, −*z*+1; (iii) −*x*, −*y*+1, −*z*+1; (iv) *x*−1, *y*, *z*; (v) *x*+1, *y*, *z*; (vi) −*x*+1, −*y*, −*z*+1; (vii) −*x*, −*y*+1, −*z*.
Bond valence parameters: Li^+: 1.466 Å, Na^+: 1.803 Å, B^{3+}: 1.371 Å, P^{5+}: 1.617 Å.

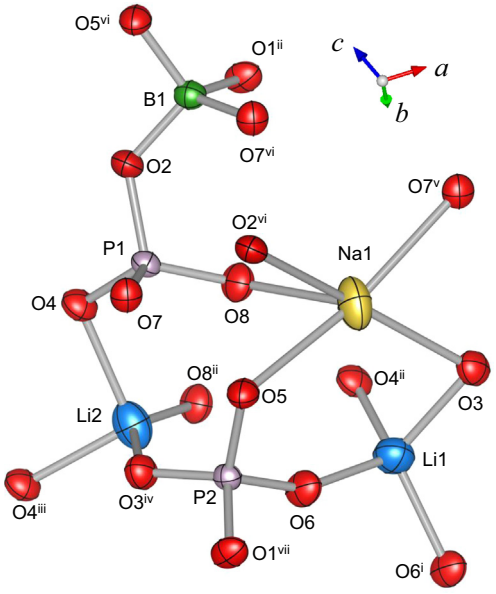

Fig. 1. An atomic arrangement around Li, Na, B and P atoms in the structure of $Li_2NaBP_2O_8$. Displacement ellipsoids are drawn at the 90% probability level. Symmetry codes: (i) −*x*+1, −*y*+1, −*z*; (ii) −*x*+1, −*y*+1, −*z*+1; (iii) −*x*, −*y*+1, −*z*+1; (iv) *x*−1, *y*, *z*; (v) *x*+1, *y*, *z*; (vi) −*x*+1, −*y*, −*z*+1; (vii) −*x*, −*y*+1, −*z*.

Table 3
Anisotropic displacement parameters (U_{ij}/Å^2) for $Li_2NaBP_2O_8$.

Atom	Site	U_{11}	U_{22}	U_{33}	U_{23}	U_{13}	U_{12}
Li1	2*i*	0.0143(14)	0.0179(14)	0.0131(14)	0.0042(12)	0.0023(11)	−0.0004(11)
Li2	2*i*	0.0129(14)	0.0155(14)	0.0203(15)	−0.0006(12)	0.0047(12)	−0.0015(11)
Na1	2*i*	0.0137(4)	0.0235(4)	0.0277(4)	0.0047(3)	0.0101(3)	−0.0014(3)
B1	2*i*	0.0087(8)	0.0088(8)	0.0088(8)	0.0022(6)	0.0018(6)	0.0000(6)
P1	2*i*	0.0072(2)	0.0071(2)	0.0078(2)	0.00151(15)	0.00195(15)	0.00086(14)
P2	2*i*	0.0068(2)	0.0071(2)	0.0072(2)	0.00156(15)	0.00142(15)	−0.00062(14)
O1	2*i*	0.0108(6)	0.0121(6)	0.0080(5)	0.0018(4)	0.0003(4)	−0.0035(4)
O2	2*i*	0.0084(5)	0.0134(6)	0.0100(5)	0.0047(4)	0.0022(4)	0.0025(4)
O3	2*i*	0.0113(6)	0.0124(6)	0.0112(6)	0.0020(4)	0.0044(5)	0.0020(4)
O4	2*i*	0.0110(6)	0.0099(5)	0.0120(6)	0.0023(4)	0.0036(5)	0.0032(4)
O5	2*i*	0.0108(6)	0.0093(5)	0.0112(5)	0.0040(4)	0.0045(4)	0.0018(4)
O6	2*i*	0.0111(6)	0.0126(6)	0.0128(6)	0.0036(5)	0.0021(5)	−0.0042(4)
O7	2*i*	0.0097(6)	0.0099(5)	0.0089(5)	0.0001(4)	0.0031(4)	−0.0009(4)
O8	2*i*	0.0117(6)	0.0118(6)	0.0144(6)	0.0029(5)	0.0050(5)	−0.0023(4)

of the four-membered rings composed of two PO_4 and two BO_4 tetrahedra. The fundamental building unit (FBU) can be expressed by the description of Ewald et al. as $6\square:\square<4\square>\square$. The Li atoms in Li1 site are replaced with Na atoms in $Li_2NaBP_2O_8$. The lattice volume of $Li_2NaBP_2O_8$ (294.04(3) $Å^3$) is larger than that of $Li_3BP_2O_8$ (279.06(5) $Å^3$) due to the bigger size of Na ions. Fig. 4 shows the Li–Li atom arrangement with the site distances on the a–c plane ($b\sim0.5$) of $Li_2NaBP_2O_8$ with those of $Li_3BP_2O_8$ in parentheses. Zigzag chains of Li atoms run in the $[a+c]$ direction.

In the crystal structure of $Na_3BP_2O_8$ (monoclinic, space group: $C2/c$ (No. 15)) reported by Xiong et al., chains which are parallel to each other in one monolayer rotate by about 100° in relation to the

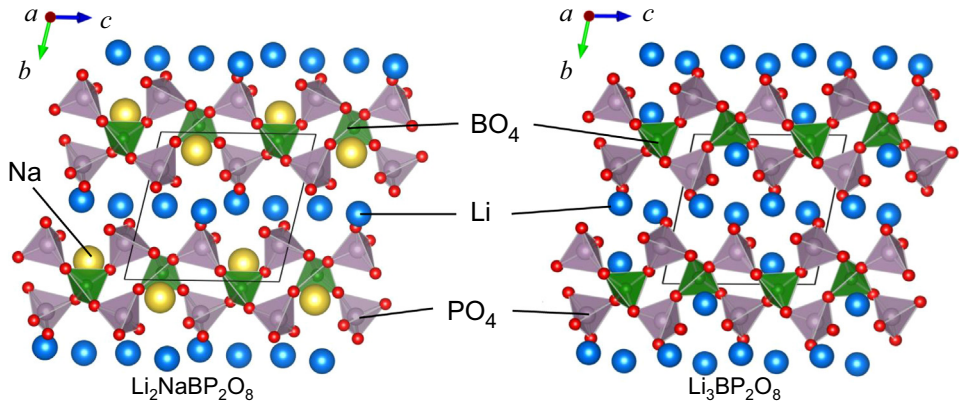

Fig. 2. Projective views of the crystal structures of $Li_2NaBP_2O_8$ and $Li_3BP_2O_8$ along the a axis.

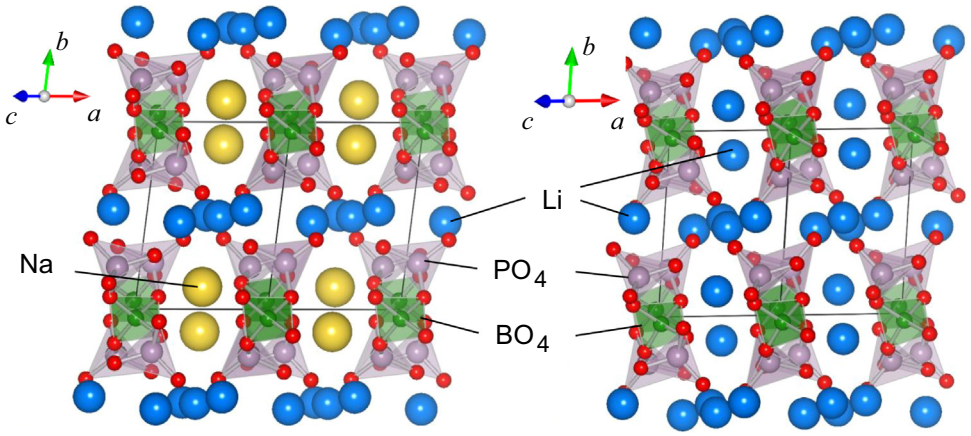

Fig. 3. Projective views of the crystal structures of $Li_2NaBP_2O_8$ and $Li_3BP_2O_8$ in the [1 0 1] direction.

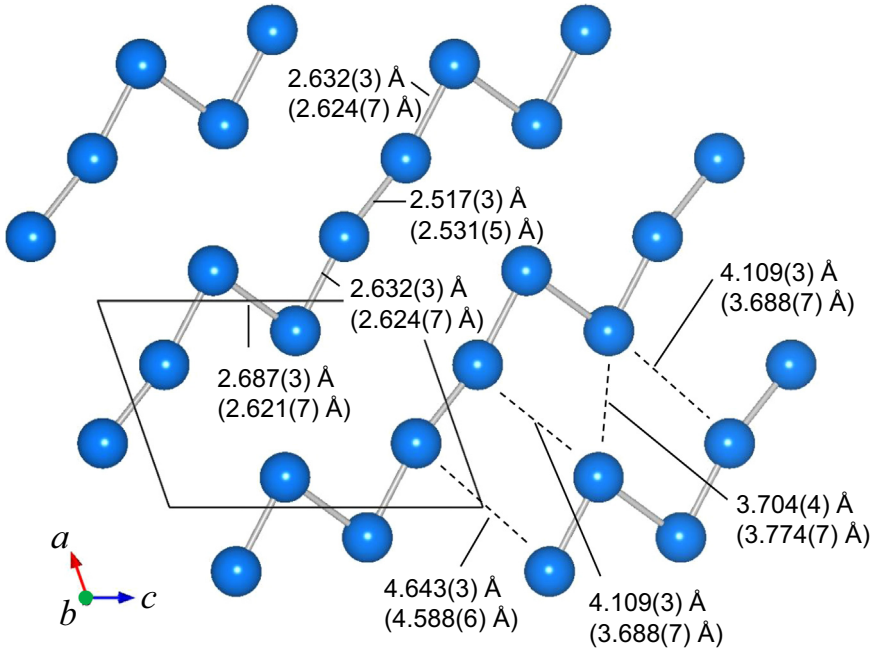

Fig. 4. Projective views of the Li layers of $Li_2NaBP_2O_8$ and $Li_3BP_2O_8$ with Li–Li interatomic distances. (The Li–Li distances of $Li_3BP_2O_8$ are shown in parentheses).

chains in the neighboring layer [13]. $LiK_2BP_2O_8$, having the same B:P ratio, crystallizes in a different structure in which two-dimensional layers of $^2_\infty[BP_2O_8]^{3-}$ are composed of BO_4 and PO_4 tetrahedra.

3.2. Crystal structure of $LiNa_2B_5P_2O_{14}$

$LiNa_2B_5P_2O_{14}$ crystalizes in a monoclinic unit cell (a=8.208(3) Å, b=9.151(3) Å, c=8.349(3) Å, β=115.709(7)°). The possible space groups of $P2_1$ and $P2_1/m$ were chosen from the systematic extinctions. An initial structure model was obtained with the space group $P2_1/m$ (No. 11) by the direct method and was improved by relabeling some atoms and by searching for missing atoms from the results of differential Fourier synthesis. Finally, the crystal structure was determined by refinement with an $R1$-value (2σ) of 4.24%. The results of structure analysis, atomic coordinates, anisotropic displacement parameters and selected bond lengths of $LiNa_2B_5P_2O_{14}$ are listed in Tables 1 and 5–7. Fig. 5 shows the coordination environment of $LiNa_2B_5P_2O_{14}$ using the refined structural parameters.

Li1, Na1, Na2, B1–B5, O5–O10 sites are at special positions of 2*e* (x, 1/2, z). The others are at the general positions. B4 and B5 atoms are coordinated by three O atoms and form boron-centered triangles [BO_3]. B1, B2, B3 and P1 are tetrahedrally coordinated by four O atoms. Li1 atoms are coordinated by four O atoms, Na1 atoms by seven O atoms, and Na2 atoms by five. The B1–O distances are in the range of 1.424(4)–1.526(3) Å, B2–O distances 1.427(4)–1.475(3) Å, B3–O distances 1.419(4)–1.513(3) Å, B4–O distances 1.349(4)–1.393(4) Å, B5–O distances 1.346(5)–1.393(5) Å, P1–O distances 1.480(2)–1.5511(18), Li1–O distances 1.895(6)–2.017(6) Å, Na1–O distances 2.282(3)–2.655(3) Å and Na2–O distances 2.312(3)–2.499(2) Å. The values of BVSs were Li1:1.04, Na1:1.09, Na2:1.02, B1:3.03, B2:3.14, B3:3.11, B4:3.02, B5:3.07 and P1:5.06. These are comparable with the valences of the elements.

Table 5
Atomic coordinates and isotropic and equivalent isotropic displacement parameters (U_{eq}) for $LiNa_2B_5P_2O_{14}$.

Atom	Site	x	y	z	U_{eq}[a](Å^2)
Li1	2*e*	0.0144(8)	0.25	0.7154(8)	0.0183(13)
Na1	2*e*	0.6034(2)	0.25	0.53499(19)	0.0260(4)
Na2	2*e*	0.8341(2)	0.25	0.95832(19)	0.0255(4)
B1	2*e*	0.2656(5)	0.25	0.5453(5)	0.0124(8)
B2	2*e*	0.2806(5)	0.25	0.0982(5)	0.0123(8)
B3	2*e*	0.9490(5)	0.25	0.3494(5)	0.0120(8)
B4	2*e*	0.4151(5)	0.25	0.8845(5)	0.0147(8)
B5	2*e*	0.6105(5)	0.25	0.1995(5)	0.0157(8)
P1	4*f*	0.15342(8)	0.05756(7)	0.27310(8)	0.0120(2)
O1	4*f*	0.2981(2)	0.11792(19)	0.4514(2)	0.0136(4)
O2	4*f*	0.0322(2)	0.6182(2)	0.7508(2)	0.0196(4)
O3	4*f*	0.1859(3)	0.1187(2)	0.1168(2)	0.0266(5)
O4	4*f*	0.1555(2)	0.6040(2)	0.2673(2)	0.0176(4)
O5	2*e*	0.4104(3)	0.25	0.7209(3)	0.0158(5)
O6	2*e*	0.0849(3)	0.25	0.5273(3)	0.0127(5)
O7	2*e*	0.2656(3)	0.25	0.9166(3)	0.0127(5)
O8	2*e*	0.4630(3)	0.25	0.2318(3)	0.0233(7)
O9	2*e*	0.7726(3)	0.25	0.3418(3)	0.0184(6)
O10	2*e*	0.5881(3)	0.25	0.0243(3)	0.0194(6)

[a] $U_{eq}=(\sum_i \sum_j U_{ij}\, a_i^* \cdot a_j^*\, a_i \cdot a_j)/3$.

Table 7
Selected bond lengths and bond valence sums (V_i) for $LiNa_2B_5P_2O_{14}$.

Li1–O6	1.895(6)	Na1–O8	2.282(3)
Li1–O4^{i}	1.981(5)	Na1–O4^{iii}	2.364(2)
Li1–O4^{ii}	1.981(5)	Na1–O4^{iv}	2.364(2)
Li1–O7	2.017(6)	Na1–O9	2.545(3)
V_{Li1}	1.04	Na1–O1	2.590(2)
		Na1–O1^{v}	2.590(2)
		Na1–O5	2.655(3)
		V_{Na1}	1.09
Na2–O10^{vi}	2.312(3)	B1–O6	1.424(4)
Na2–O4^{iii}	2.341(2)	B1–O5	1.432(4)
Na2–O4^{iv}	2.341(2)	B1–O1	1.526(3)
Na2–O2^{vii}	2.499(2)	B1–O1^{v}	1.526(3)
Na2–O2^{viii}	2.499(2)	V_{B1}	3.03
V_{Na2}	1.02		
B2–O8	1.427(4)	B3–O6^{ix}	1.419(4)
B2–O7^{vi}	1.467(4)	B3–O9	1.421(4)
B2–O3	1.475(3)	B3–O2^{iii}	1.513(3)
B2–O3^{v}	1.475(3)	B3–O2^{iv}	1.513(3)
V_{B2}	3.14	V_{B3}	3.11
B4–O5	1.349(4)	B5–O9	1.346(5)
B4–O7	1.365(4)	B5–O8	1.349(5)
B4–O10^{vi}	1.393(4)	B5–O10	1.393(5)
V_{B4}	3.02	V_{B5}	3.07
P1–O4	1.480(2)		
P1–O3	1.5455(19)		
P1–O1	1.5483(17)		
P1–O2	1.5511(18)		
V_{P1}	5.06		

Symmetry codes: (i) $-x$, $-y+1$, $-z+1$; (ii) $-x$, $y-1/2$, $-z+1$; (iii) $-x+1$, $-y+1$, $-z+1$; (iv) $-x+1$, $y-1/2$, $-z+1$; (v) x, $-y+1/2$, z; (vi) x, y, $z+1$; (vii) $-x+1$, $-y+1$, $-z+2$; (viii) $-x+1$, $y-1/2$, $-z+2$; (ix) $x+1$, y, z.

Table 6
Anisotropic displacement parameters (U_{ij}/Å^2) for $LiNa_2B_5P_2O_{14}$.

Atom	Site	U_{11}	U_{22}	U_{33}	U_{23}	U_{13}	U_{12}
Li1	2*e*	0.014(3)	0.025(3)	0.018(3)	0	0.009(3)	0
Na1	2*e*	0.0174(8)	0.0437(11)	0.0140(8)	0	0.0041(7)	0
Na2	2*e*	0.0207(8)	0.0435(11)	0.0146(8)	0	0.0097(7)	0
B1	2*e*	0.0099(17)	0.021(2)	0.0057(17)	0	0.0025(15)	0
B2	2*e*	0.0100(17)	0.020(2)	0.0086(18)	0	0.0054(16)	0
B3	2*e*	0.0078(17)	0.019(2)	0.0076(18)	0	0.0016(15)	0
B4	2*e*	0.0094(18)	0.026(2)	0.0082(19)	0	0.0032(16)	0
B5	2*e*	0.0078(17)	0.028(2)	0.0090(19)	0	0.0017(16)	0
P1	4*f*	0.0136(3)	0.0113(4)	0.0109(4)	0.0007(2)	0.0052(3)	0.0001(2)
O1	4*f*	0.0118(8)	0.0170(9)	0.0109(8)	−0.0008(7)	0.0039(7)	0.0015(7)
O2	4*f*	0.0112(9)	0.0228(10)	0.0179(10)	0.0084(7)	−0.0002(8)	−0.0043(7)
O3	4*f*	0.0414(12)	0.0275(11)	0.0135(9)	−0.0041(8)	0.0143(9)	−0.0193(9)
O4	4*f*	0.0191(9)	0.0114(9)	0.0224(10)	0.0003(7)	0.0090(8)	0.0000(7)
O5	2*e*	0.0081(11)	0.0296(15)	0.0092(12)	0	0.0033(10)	0
O6	2*e*	0.0080(11)	0.0230(14)	0.0079(12)	0	0.0044(10)	0
O7	2*e*	0.0078(11)	0.0243(14)	0.0063(11)	0	0.0034(10)	0
O8	2*e*	0.0072(12)	0.055(2)	0.0075(12)	0	0.0031(11)	0
O9	2*e*	0.0082(12)	0.0368(16)	0.0108(12)	0	0.0047(11)	0
O10	2*e*	0.0100(12)	0.0409(17)	0.0078(12)	0	0.0045(10)	0

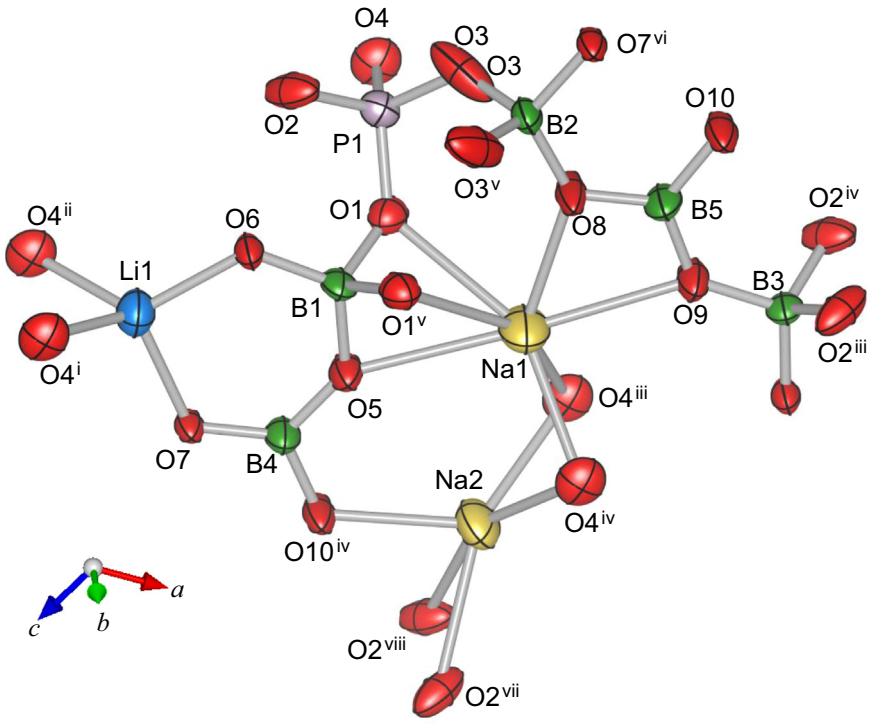

Fig. 5. Atomic arrangement around Li, B, and P atoms in the structure of $LiNa_2B_5P_2O_{14}$. Displacement ellipsoids are drawn at the 90% probability level. Symmetry codes: (i) $-x$, $-y+1$, $-z+1$; (ii) $-x$, $y-1/2$, $-z+1$; (iii) $-x+1$, $-y+1$, $-z+1$; (iv) $-x+1$, $y-1/2$, $-z+1$; (v) x, $-y+1/2$, z; (vi) x, y, $z+1$; (vii) $-x+1$, $-y+1$, $-z+2$; (viii) $-x+1$, $y-1/2$, $-z+2$; (ix) $x+1$, y, z.

Fig. 6 shows the crystal structure of $LiNa_2B_5P_2O_{14}$. Two-dimensional sheets of $^2_\infty[B_5P_2O_{14}]^{3-}$ are formed by linkage of BO_3, BO_4, and PO_4 on the a–c plane, and stacked in the direction of the b axis. The FBU of $LiNa_2B_5P_2O_{14}$ framed by two BO_3, three BO_4, and two PO_4 formed by linkage of BO_3, BO_4, and PO_4 is represented by 5□2Δ:[⟨□2Δ⟩]□|□|□|□|. Two BO_3 triangles and one BO_4 tetrahedron which form a ring of ⟨2Δ□⟩ are connected with other BO_4 tetrahedra and PO_4 tetrahedron, respectively. A large triangular space is created by linkage of three FBUs in the sheet. Two Na atoms and one Li atom are in each triangular space of the sheet. Such a sheet structure has not been previously reported in systems of Li_2O–B_2O_3–P_2O_5 and Na_2O–B_2O_3–P_2O_5. This sheet structure is probably stabilized by the combination of Li and Na atoms. In our previous study, we revealed for the first time that $Li_2B_3PO_8$ is an example of the 2D sheet structure composed of a mixture of BO_3 triangles, BO_4 tetrahedra and PO_4 tetrahedra. The crystal structure of $LiNa_2B_5P_2O_{14}$ is a second example.

The value of the Madelung part of lattice energy (MAPLE) for $LiNa_2B_5P_2O_{14}$ calculated with the structure parameters was −103,900 kJ/mol, which is almost identical to the value of −103,100 kJ/mol (difference $\Delta=0.8\%$) of the MAPLEs: Li_2O −3500 kJ/mol [22], Na_2O −2900 kJ/mol [23], B_2O_3 −21,900 kJ/mol [24], and P_2O_5 −43,700 kJ/mol [25] with the formula $LiNa_2B_5P_2O_{14}=1/2\ Li_2O+Na_2O+5/2\ B_2O_3+P_2O_5$.

3.3. Electrical resistivities

As shown in Fig. 7(a), all powder XRD peaks of the $Li_2NaBP_2O_8$ polycrystalline bulk sample were indexed with the cell parameters obtained by the single crystal X-ray diffraction. The most part of the powder XRD pattern measured for the $LiNa_2B_5P_2O_{14}$ bulk sample could be explained with the structure analyzed by single crystal XRD analysis, and small amounts of BPO_4 and an unidentified phase were contained.

The results of impedance measurement at 583, 593 and 606 K for the polycrystalline bulk sample of $Li_2NaBP_2O_8$ single phase (diameter: 6.05 mm, thickness: 1.18 mm) are shown in Fig. 8. A total electrical

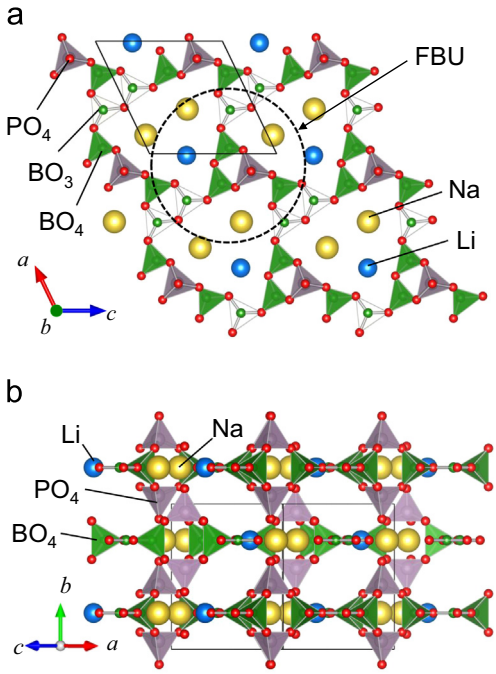

Fig. 6. Projective views of the crystal structure of $LiNa_2B_5P_2O_{14}$ along the b axis (a) and in the [1 0 1] direction ($y=0$–0.5) (b).

resistance of $Li_2NaBP_2O_8$ was 73 kΩ at 583 K, which was converted to a conductivity of 1.7×10^{-6} S cm^{-1}. Fig. 9 shows a logarithmic plot of the electrical conductivities measured by the AC impedance method as a function of reciprocal measurement temperatures. The conductivities of $Li_3BP_2O_8$ and $Li_2B_3PO_8$ reported in the previous studies [7,8] are also plotted in Fig. 9. The electrical conductivities of the $Li_2NaBP_2O_8$ sample were lower than those of $Li_3BP_2O_8$ in the measured temperature range. The activation energy of $Li_2NaBP_2O_8$ (140 kJ/mol) was higher than that of $Li_3BP_2O_8$ (72 kJ/mol).

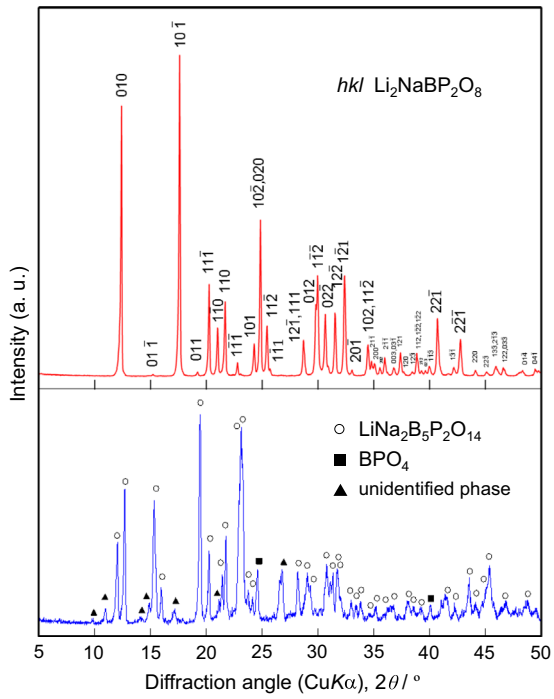

Fig. 7. XRD patterns of the powdered $Li_2NaBP_2O_8$ and $LiNa_2B_5P_2O_{14}$ bulk samples.

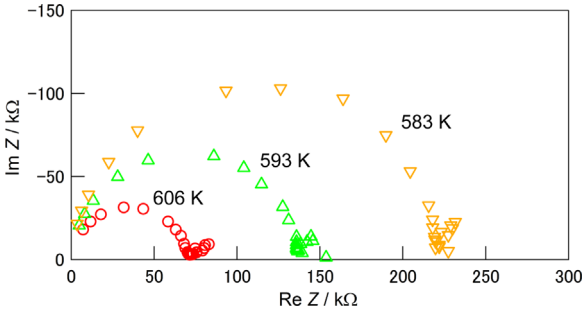

Fig. 8. Complex impedance plots for a polycrystalline $Li_2NaBP_2O_8$ bulk sample at 583–606 K.

$Li_3BP_2O_8$ [7] and $Li_2NaBP_2O_8$ are isotypic and have one-dimensional zigzag Li^+ ion chains in the *a*–*c* plane between the slabs of Li^+/Na^+ ions and $^1_\infty[BP_2O_8]^{3-}$ chains. The average distances of intra- and inter-Li–Li sites of the zigzag chains increased from 2.592 to 2.612 Å and from 3.935 to 4.141 Å, respectively, by substitution of Na^+ for Li^+ in the slabs (Fig. 4). Such site distance increases are one of the reasons for the reduction of Li^+ ion conductivity and the increase of activation energy.

The resistance of the $LiNa_2B_5P_2O_{14}$ sample was over 10 MΩ and out of the measurement range of the impedance analyzer. This indicates that migration of Li^+ and Na^+ ions to the neighboring sites of the triangular space in the $^2_\infty[B_5P_2O_{14}]^{3-}$ sheets of $LiNa_2B_5P_2O_{14}$ is difficult. Similar high resistivity was observed for $Li_2B_3PO_8$, having Li^+ ions in the space in the $^2_\infty[B_3PO_8]^{2-}$ sheets.

4. Summary

Single crystals of novel quintenary oxides, $Li_2NaBP_2O_8$ and $LiNa_2B_5P_2O_{14}$, were synthesized by cooling of the samples from 873 K and from 883 K, respectively. $Li_2NaBP_2O_8$, isotypic with $Li_3BP_2O_8$, crystallizes in a triclinic cell ($P\bar{1}$). B and P atoms are located at tetrahedral sites of O atoms and form $^1_\infty[BP_2O_8]^{3-}$ chains by sharing the vertex oxygen

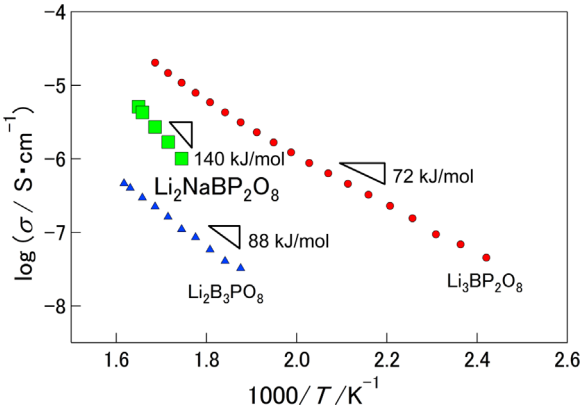

Fig. 9. Arrhenius plots of the conductivities of $Li_2NaBP_2O_8$, $Li_3BP_2O_8$ and $Li_2B_3PO_8$ measured by the AC impedance method.

atoms of the tetrahedra. $LiNa_2B_5P_2O_{14}$ (monoclinic $P2_1/m$), is composed of $^2_\infty[B_5P_2O_{14}]^{3-}$ sheets. The electric conductivity of 1.7×10^{-6} S cm^{-1} was measured for $Li_2NaBP_2O_8$ at 583 K by the AC impedance method.

Appendix A. Supporting information

Supplementary data associated with this article can be found in the online version at http://dx.doi.org/10.1016/j.jssc.2014.11.024.

References

[1] R. Kneip, G. Gozel, B. Eisenmann, C. Rohr, M. Asbrand, M. Kizikyalli Angew. Chem. Int. Ed. Engl. 33 (1994) 749–751.
[2] R. Kniep, H. Engelhardt, C. Hauf, Chem. Mater. 10 (1998) 2930–2934.
[3] O.A. Gurbanova, E.L. Belokoneva, Crystallogr. Rep. 52 (2007) 624.
[4] B. Ewald, Y.X. Huang, R. Kniep, Z. Anorg. Allg. Chem. 633 (2007) 1517–1540.
[5] (a) D. Zhao, W. Cheng, H. Zhang, S. Huang, Z. Xie, W. Zhang, S. Yang, Inorg. Chem. 48 (2009) 6623–6629;
(b) Y. Wang, S. Pan, M. Zhang, S. Han, X. Su, L. Dong, CrystEngComm 15 (2013) 4956–4962;
(c) H. Li, Y. Zhao, S. Pan, H. Wu, H. Yu, F. Zhang, Z. Yang, K.R. Poeppelmeier, Eur. J. Inorg. Chem. (2013) 3185–3190;
(d) A.A. Babaryk, I.V. Odynets, N.S. Slobodyanik, V.N. Baumer, S. Khainakov, CrystEngComm 14 (2012) 5071–5077;
(e) Y. Wang, S. Pan, S. Huang, L. Dong, M. Zhang, S. Han, X. Wang, Dalton Trans. 43 (2014) 12886–12893;
(f) Y. Wang, S. Han, B. Zhang, L. Dong, M. Zhang, Z. Yang, CrystEngComm 16 (2014) 6848–6851.
[6] T.Y. Tien, F.A. Hymmel, J. Am. Ceram. Soc. 44 (1961) 391–393.
[7] T. Hasegawa, H. Yamane, Dalton Trans. 43 (2014) 2294–2300.
[8] T. Hasegawa, H. Yamane, Dalton Trans. 43 (2014) 14525–14528.
[9] C. Hauf, T. Friedrich, R. Kniep, Z. Kristallogr. 210 (1995) 446 (–446).
[10] C. Hauf, A. Yilmaz, M. Kizilyalli, R. Kneip, J. Solid State Chem. 140 (1998) 154–156.
[11] Z. Lin, Y. Wu, P. Fu, S. Pan, Z. Lin, C. Chen, J. Cryst. Growth 255 (2003) 119–122.
[12] H. Rahab, D. Ouadjaout, A. Manseri, O. Viraphong, J.P. Chaminade, J. Cryst. Growth 303 (2007) 629–631.
[13] D. Xiong, H. Chen, X. Yang., J. Zhao, J. Solid State Chem. 180 (2007) 233–239.
[14] Y. Wang, S. Pan., Y. Shi, Chem. Eur. J. 18 (2012) 12046–12051.
[15] RAPID-AUTO, Rigaku Corporation, Tokyo, 2005.
[16] T. Higashi, NUMABS—Numerical Absorption Correction, Rigaku Corporation, Tokyo, 1999.
[17] L.J. Farrugia, J. Appl. Crystallogr 32 (1999) 837–838.
[18] M.C. Burla, R. Caliandro, M. Camalli, B. Carrozzini, G.L. Cascarano, L. De Caro, C. Giacovazzo, G. Polidori, R. Spagna, J. Appl. Crystallogr 38 (2005) 381–388.
[19] G.M. Sheldrick, Acta Crystallogr A64 (2008) 112–122.
[20] K. Momma, F. Izumi, J. Appl. Crystallogr 41 (2008) 653–658.
[21] N.E. Brese, M. O'Keeffe, Acta Crystallogr B47 (1991) 192–197.
[22] E. Zintl, A. Harder, B. Dauth, Z. Elktrochem 40 (1934) 588–593.
[23] E. Zintl, H.H.v. Baumbach, Z. Anorg. Anorg. Allg. Chem 198 (1931) 88–101.
[24] G.E. Gurr, P.W. Montgomery, C.D. Knutson, B.T. Gorres, Acta Crystallogr B26 (1970) 906–915.
[25] C.H. Macgillavry, H.C.J. Dedecker, L.M. Nijland, Nature 164 (1949) 448–449.